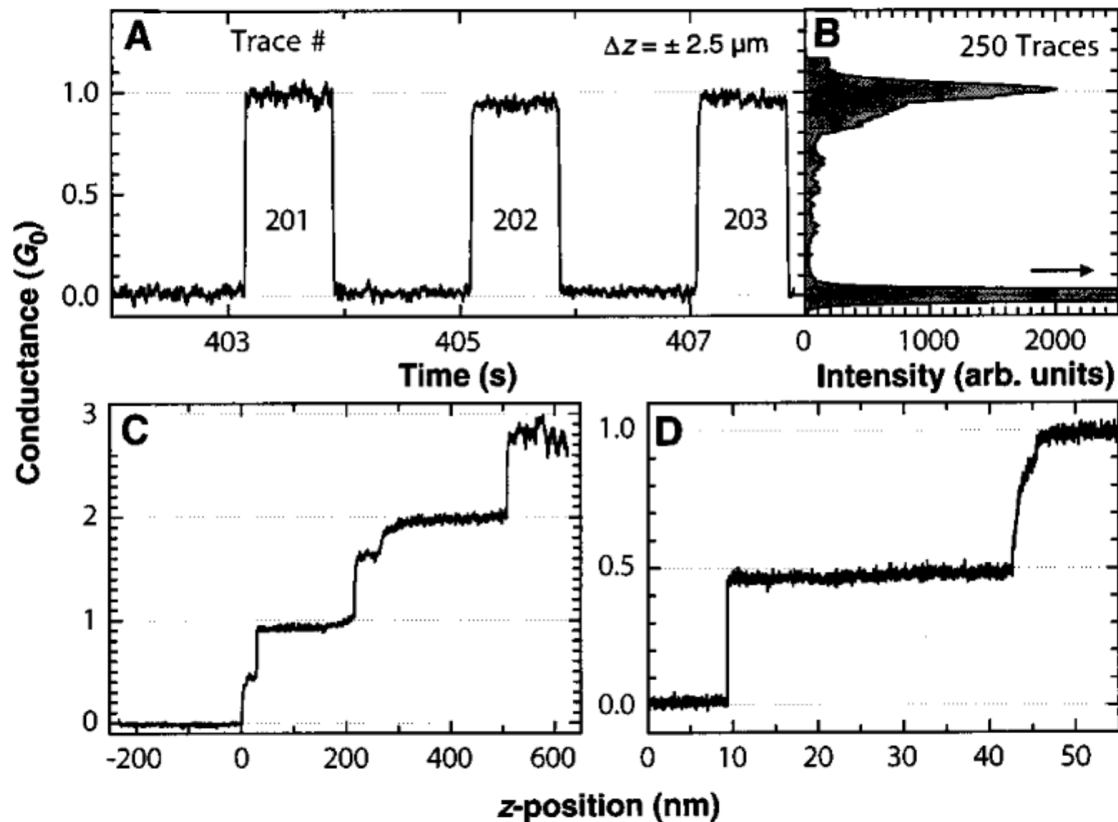


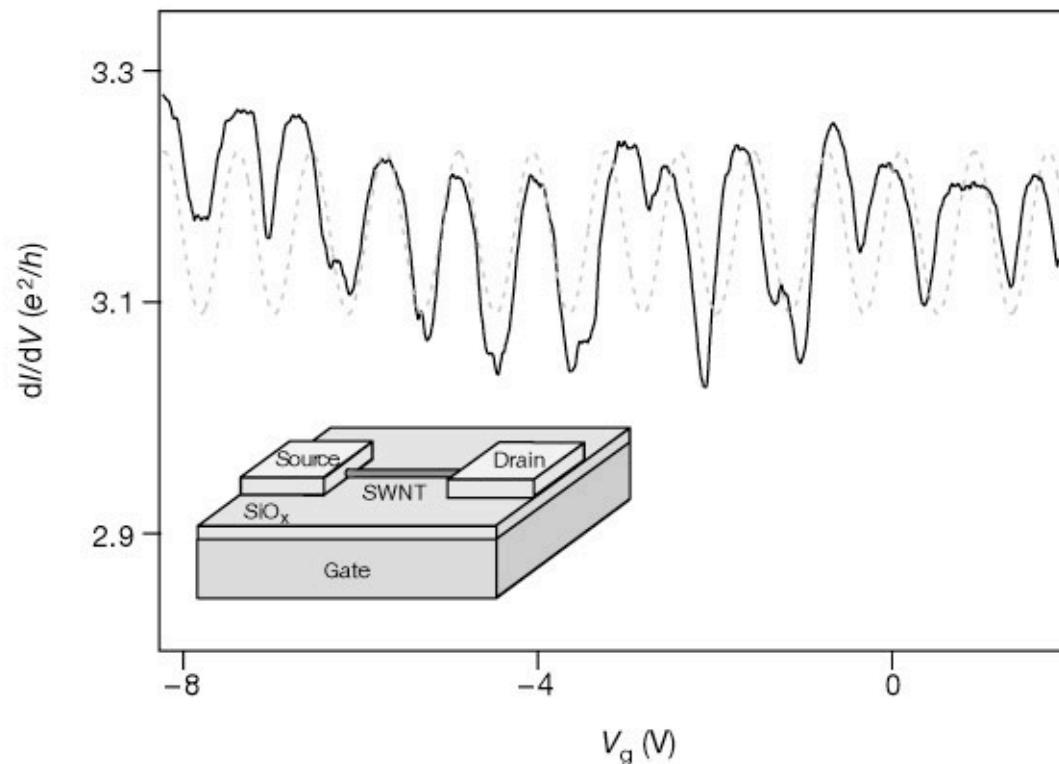
# Quantum Transport

PH671 - Transport

Carbon nanotube conductance measurements. (A) Conductance of a nanotube contact that is moved at constant speed into and out of the mercury contact as a function of time. The period of motion is 2 s and the displacement  $\approx 2.5 \mu\text{m}$ . The conductance “jumps” to  $1G_0$  and then remains constant for  $\approx 2 \mu\text{m}$  of its dipping depth. The direction of motion is then reversed and the contact is broken after  $2 \mu\text{m}$  SCIENCE VOL. 280 12 JUNE 1998 p1774

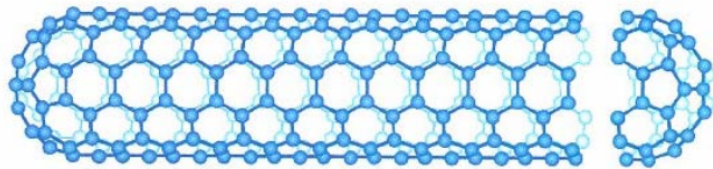
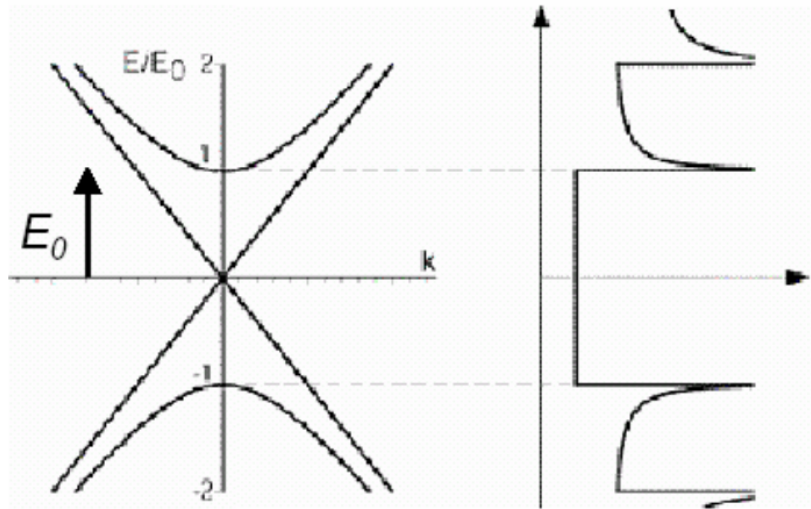


Isolated SWNTs were synthesized on a degenerately doped silicon wafer with a 1- $\mu\text{m}$  oxide layer by chemical vapour deposition. Individual SWNTs with 1-nm height were located by atomic force microscopy, and nanotube devices were fabricated by defining two Au/Cr electrodes on top of the SWNTs by electron-beam lithography. Electrical properties of nanotube devices were characterized as a function of bias voltage ( $V$ ) and  $V_g$ . The degenerately doped silicon substrate was used as a gate electrode to modulate the charge density and the Fermi-level position within the nanotubes. The dotted curve shows a sinusoidal function with the same average period as the measured data. Comparison between these two plots shows that the measured data is quasi-periodic in  $V_g$ . Inset, a schematic diagram of the SWNT device, showing a nanotube with attached leads, the insulating gate oxide and the degenerately doped silicon gate.



Type I. Metallic tubes

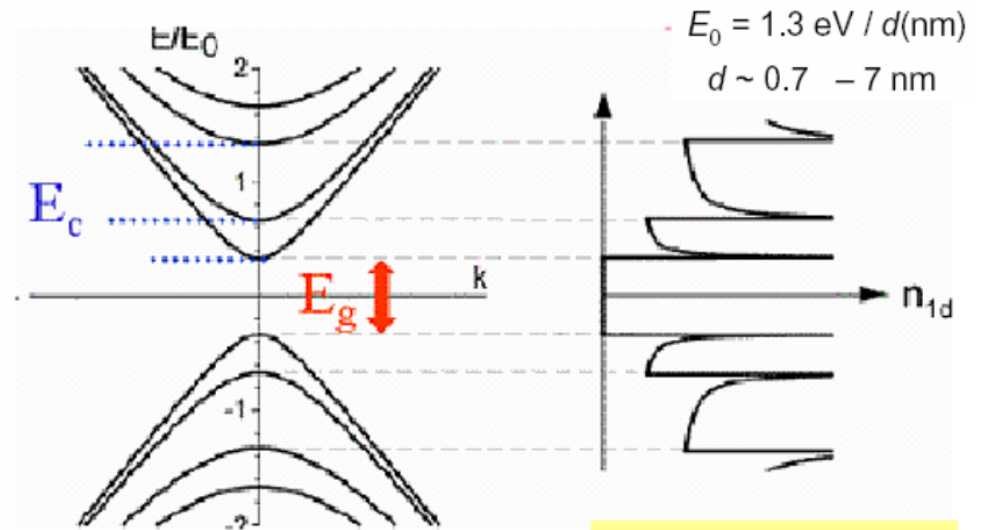
$M-N = 0$     $E_g = 0$



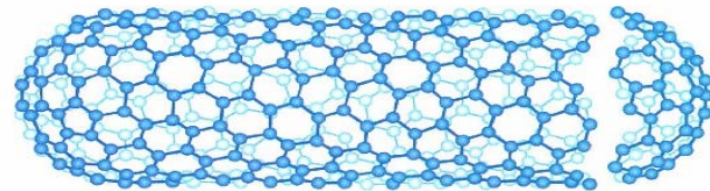
$(N, M) = (5, 5)$

Type II. Wide-gap semiconducting tubes

$M-N \neq 3p$     $E_g = 2/3 E_0$



$E_g \sim 0.5-1$  eV



$(N, M) = (10, 5)$

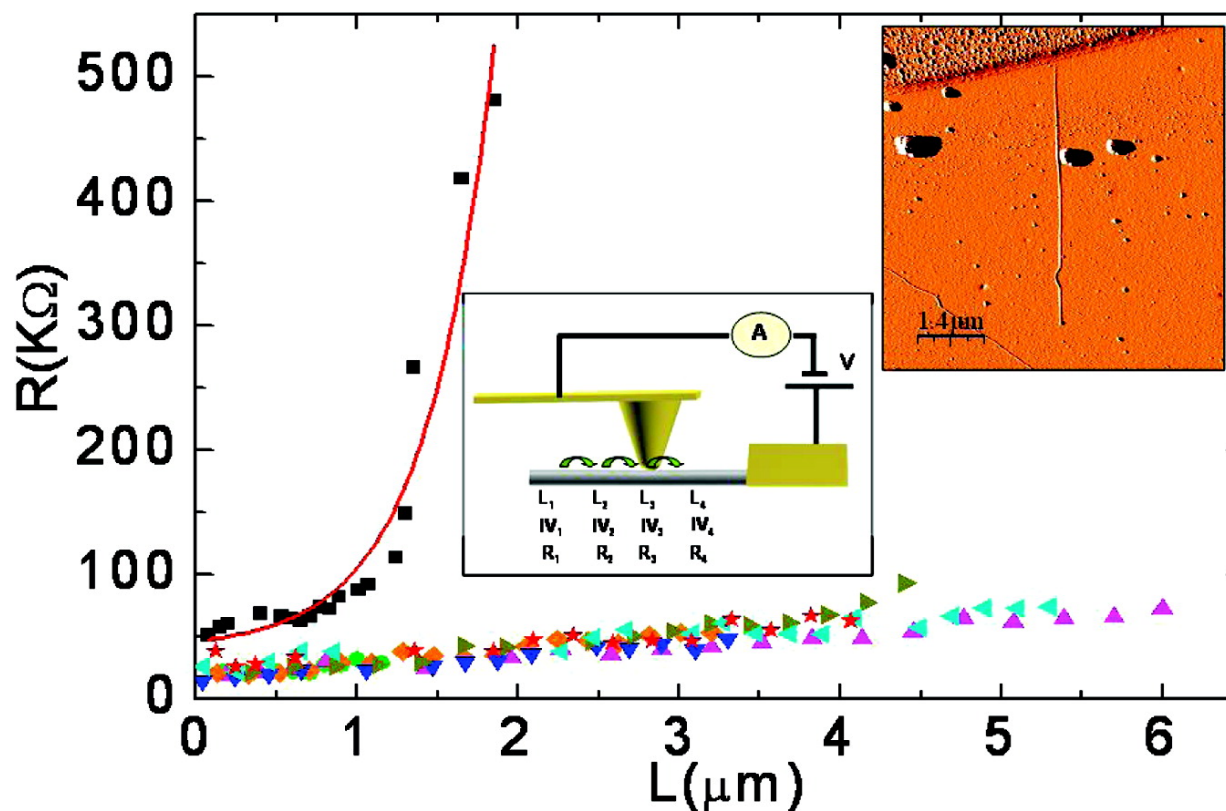


Figure 1 Experimental dependence of the low voltage resistance vs length for CVD-grown SWNTs (triangles and stars) and HipCo SWNTs (squares). The experimental set up is illustrated in the central inset of the figure. A metallic AFM tip is moved along the nanotube probing its electrical conductance as a function of the tip–electrode distance. The upper inset is an AFM image of a long nanotube partially covered with gold. The nanotubes directly grown on surface present low disorder and hence the conductance is quasiballistic; the low increment of the resistance with length is a consequence of the interaction with acoustic phonons and disorder. The HipCo SWNT presents a high density of defects resulting in an electronic transport regime governed by the Anderson localization phenomenon.

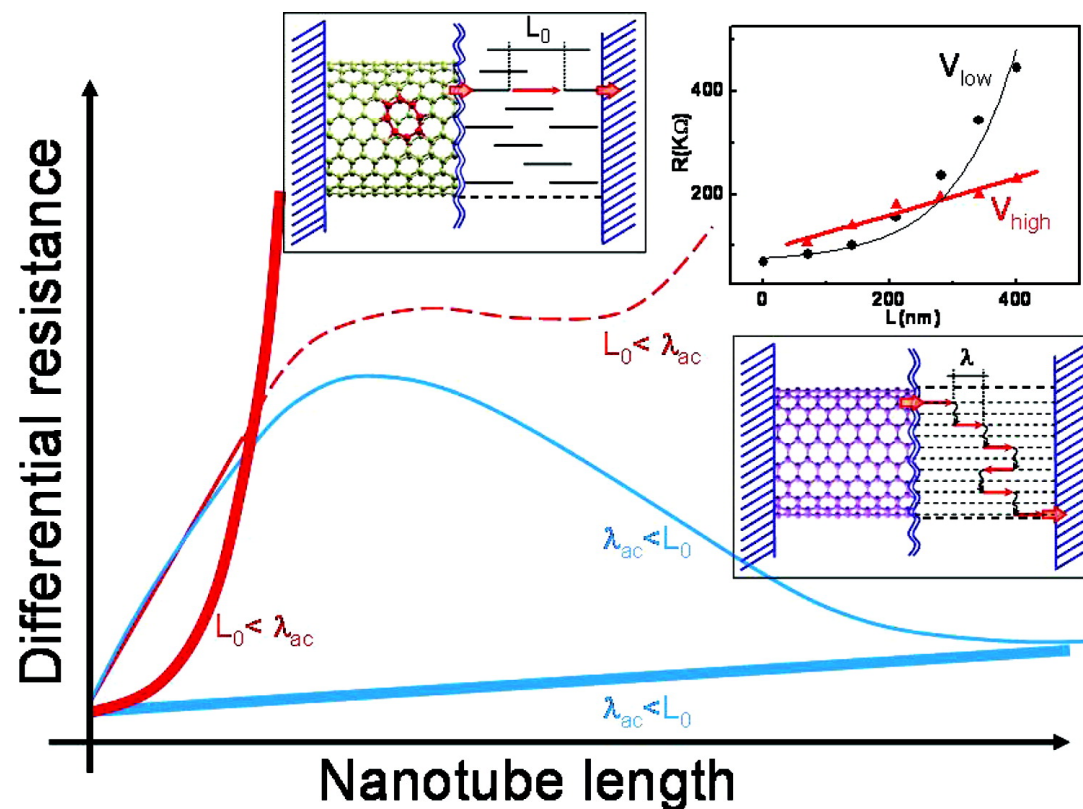
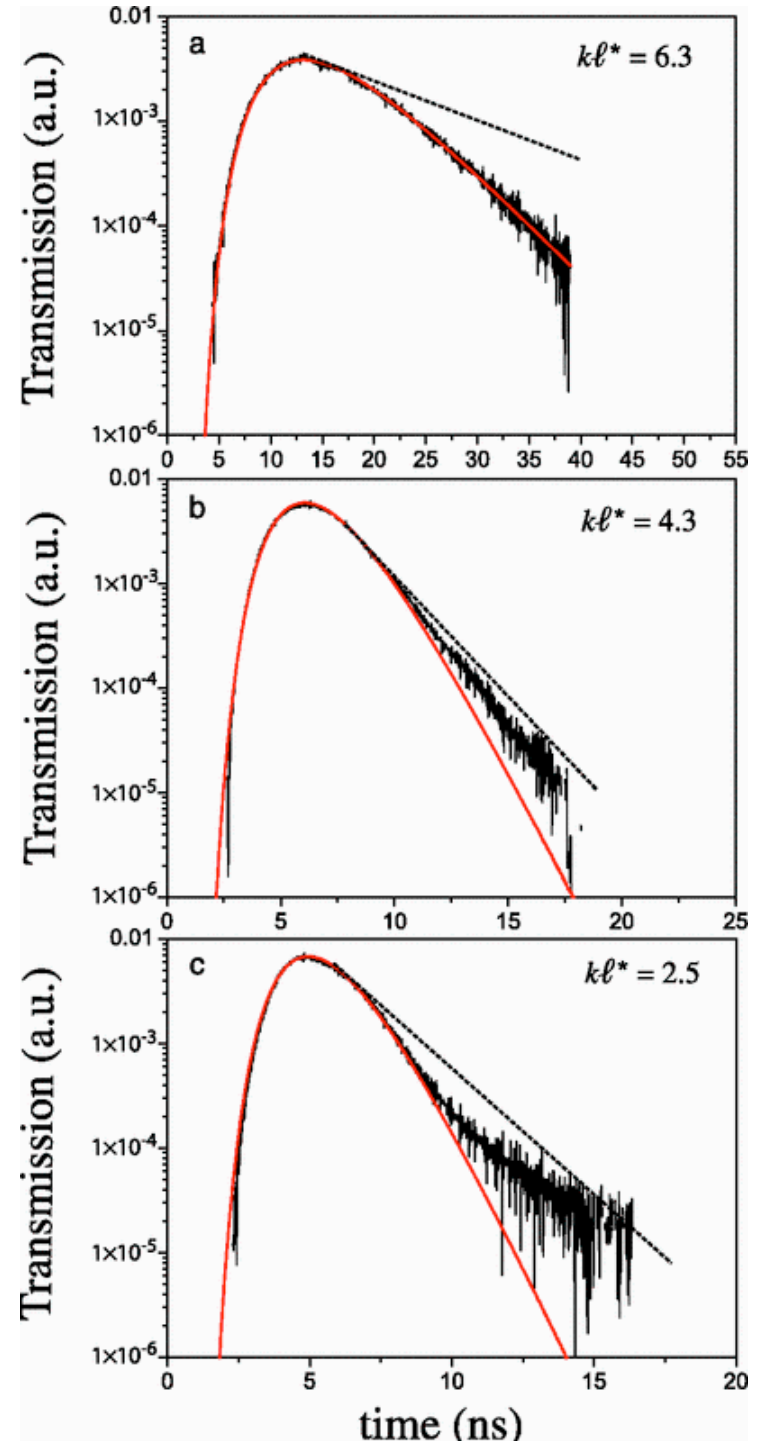
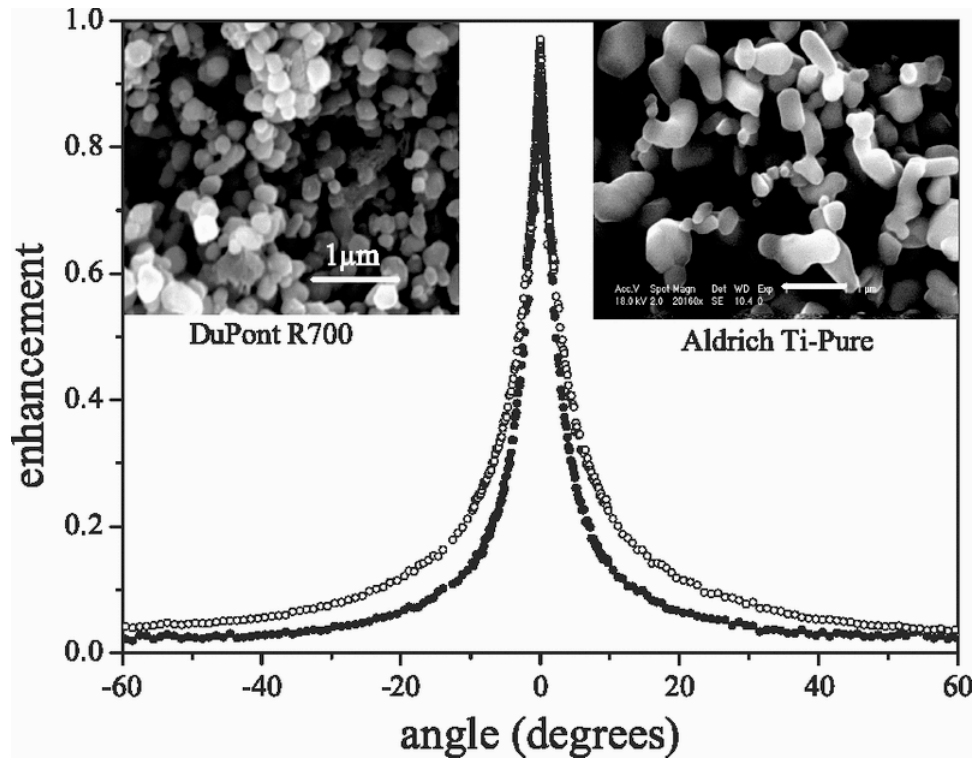


Figure 4 This figure summarizes the different electron transport regimes for SWNTs with and without defects as a function of the bias voltage and length. The thick lines apply to the low bias voltage. The thin lines apply for the high bias voltage. The blue curves are for defect-free SWNTs (lower inset) and the red ones for defected SWNTs (upper left inset). The upper right inset shows experimental  $R(L)$  at low and high bias voltages for a defected SWNT whose localization length is  $L_0 = 95$  nm.

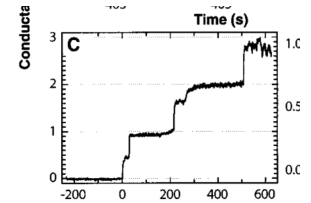
# Observation of the Critical Regime Near Anderson Localization of Light

Martin Störzer, Peter Gross, Christof M. Aegerter, and Georg Maret  
Phys. Rev. Lett. 96, 063904 – Published 15 February 2006  
DOI: <http://dx.doi.org/10.1103/PhysRevLett.96.063904>



Ballistic transport in 1d (no scattering):

$$G = \frac{2e^2}{h} N_{\text{channels}}; \quad R_{\text{res}} = \frac{1}{G} = \frac{h}{2e^2} \frac{1}{N_{\text{channels}}}$$

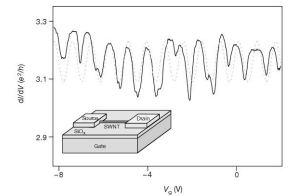


Landauer – imperfect channels

$$G = \frac{2e^2}{h} T = \frac{2e^2}{h} \sum_{i=1}^N T_i; \quad R_{\text{res}} = \frac{1}{G}$$

2 inelastic scatterers. Preserves phase coherence. Oscillations.

$$T = \frac{|t_1|^2 |t_2|^2}{1 + |r_1|^2 |r_2|^2 - 2|r_1||r_2|\cos\phi}; \quad R_{\text{res}} = \frac{h}{2e^2} \frac{1 + |r_1|^2 |r_2|^2 - 2|r_1||r_2|\cos\phi}{|t_1|^2 |t_2|^2}$$





Several energies – keep coherence but average over phase.

$$\langle R_{res} \rangle = \frac{h}{2e^2} \frac{1 + |r_1|^2 |r_2|^2}{|t_1|^2 |t_2|^2}$$

$N$  scatterers with phase-average ....

$$\langle R_{res} \rangle_{N+1} = \frac{h}{2e^2} \frac{1 + RdR}{T(1-dR)} \xrightarrow{R \rightarrow 1} \frac{h}{2e^2 T} (1 + 2dR) = \langle R_{res} \rangle_N \left( 1 + 2 \frac{dL}{\ell_e} \right)$$

...gives localization. Need low temperature to suppress phonons

$$\langle dR_{res} \rangle = \langle R_{res} \rangle 2 \frac{dL}{\ell_e} \Rightarrow \langle R_{res} \rangle = \frac{h}{2e^2} e^{\frac{2L}{\ell_e}}$$

2 elastic scatterers. No phase coherence. Add classically.

$$T = \frac{|t_1|^2 |t_2|^2}{1 - |r_1|^2 |r_2|^2}; \quad R_{res} = \frac{h}{2e^2} \frac{1 - |r_1|^2 |r_2|^2}{|t_1|^2 |t_2|^2} = \frac{h}{2e^2} \left( 1 + \frac{|r_1|^2}{|t_1|^2} + \frac{|r_2|^2}{|t_2|^2} \right)$$

$N$  elastic scatterers. No phase coherence. Add classically....

$$R_{res} = \frac{h}{2e^2} \left( 1 + N \frac{|r|^2}{|t|^2} \right) \xrightarrow{R=T=1/2} \frac{h}{2e^2} (1 + N)$$

...gives ohmic behavior - no localization.